Transient Thermal Stresses and Stress Intensity Factors Induced by Thermal Stratification in Feedwater Lines

G. Sanchez Sarmiento, E. Pardo

Empresa Nuclear Argentina de Centrales Electricas S.A., Avda. Leandro N. Alem 712, 1001 Buenos Aires, Argentina

Abstract

General analytical solutions for the thermal stresses and circumferential crack propagation in piping branches of nuclear power plants, that connect two circuits of the same fluid at different temperatures, are presented in this paper.
Under certain conditions, two regions of the fluid possessing both temperatures with a separating layer of small thickness are formed ("flow stratification"). Dimensionless analytical expressions for the steady state temperature distribution in the pipe wall and the corresponding thermal stress are here derived, in terms of the basic geometrical and physical parameters. The position and thickness of the separating layer are considered as data of the model. Stress intensity ranges at any point of the tube wall are then determined. Finally, thermally induced stress intensity factors are calculated for hipothetically inside surface cracks.

1. Introduction

In recent years recurrent failures have been observed [1-6] in certain piping branches of nuclear power plants (such as feedwater lines of primary circuit or of steam generator) that connect two circuits of the same fluid at different temperature. Thermal cycling fatigue was suggested as main cause of these failures, that consisted in the appearance of through cracks originated on the inside surface of the pipe.

Among the factors producing material fatigue, great attention has been paid in recent studies [7-14] to the formation of thermal stratification in the fluid, i.e., the presence of two regions possessing a temperature difference with a rude separating layer. This phenomenon has been experimentally verified [4,6-8] in several cases by internal temperature sensing devices, and recently confirmed by some physical [10] and computational [9] models.

The temperature gradient in the liquid produce considerable thermal stresses in the piping material which, in addition to other mechanical and thermal loads, may challenge the pipe integrity. Moreover, the significant characteristic of the thermal stratification is the oscilation of the interface, producing cyclic variation of the stresses at points near the interface that eventually leads to material fatigue.

Simplified analytical [11-14] and computational [7-8] solutions of the thermal stresses problem in the pipe wall have been obtained up to date by several authors, mainly at Kraftwerk Union A.G., F.R. of Germany. França Filho et al [15] also arrived to analytical expressions for the thermal stresses in a similar problem. In all these studies, however, very rough approximations for the temperature distribution in the tube wall is necessary to make, which in general lead to excessively conservative values of the thermal stresses.

In this paper, general analytical solutions of these thermal and thermoelastic problems

are presented. Dimensionless analytical expressions for the steady-state temperature distribution in the pipe wall and the corresponding thermal stress are here derived, in terms of basic geometrical and physical parameters of the problem. The position and thickness of the separating layer of the fluid are considered as data of the model. Stress intensity ranges at any point of the tube wall are then determined, in order to use them in the fatigue analysis of real systems. Finally, the thermally induced stress intensity factors are calculated for hypothetical inside surface cracks at the position of maximum stresses.

Dimensionless plots of general validity are presented, which may be directly applied to real situations.

2. Description of the model

The geometry of the model is indicated in figure 1. An horizontal straight pipe of infinite length (such that feedwater piping upstream of steam generator or reactor pressure vessels), contains a liquid showing a vertical distribution of temperature characterized by two portions at different constant values, separated by an horizontal layer of finite thickness ("thermal stratification").

The temperature distribution in the pipe and the thermal stress there induced are considered in the present model as dependent only on the following geometrical parameters:

r_i : internal radius of the pipe;
r_e : external radius of the pipe;
y_e : mean level of the separating layers; and
δ : the thickness of the separating layers;

and on the following physical magnitudes:

K : thermal conductivity of the pipe material;
h_i : film heat transfer coefficient of the inside surface;
h_e : film heat transfer coefficient of the outer surface;
E : Young modulus of the pipe material;
ν : Poisson's ratio of the pipe material;
α : coefficient of linear thermal expansion.

In order to obtain dimensionless analytical results of general validity for the thermal stresses, the following approximations and hypotheses are assumed:

1) Steady state regime.
2) The thermal field and stress distribution are uncoupled.
3) The temperature T_f of the fluid depends only on the vertical coordinate y as indicated in figure 1, and it is not affected by the conduction within the pipe material.
4) All the physical magnitudes K, h_i, h_e, E, ν and α are constants, i.e., independent of the temperature.
5) Room temperature outside the pipe insulation is uniform and equal to T_∞.
6) Plane sections that are normal to neutral axis at constant temperature remain planes and normals to that axis after the application of the thermal load (Classical hypotheses of Bernoulli-Euler for bending of beams). Only "Banana Effect" [14] is considered.
7) Rotations of the normal sections are small.
8) None mechanical restrictions to the expansion and bending of the tube are considered.

3. Calculation of the temperature distribution

The spatial distribution of temperature T (r,ϕ) related to the polar coordinates

indicated in figure 1 is goberned by the following steady-state heat conduction differential equation:

$$\frac{\partial^2 T}{\partial r^2} + \frac{1}{r}\frac{\partial T}{\partial r} + \frac{1}{r^2}\frac{\partial^2 T}{\partial \phi^2} = 0 \qquad (r_i < r < r_e;\ 0 \le \phi \le \pi) \tag{1}$$

subjected to the following boundary conditions:

$$K\frac{\partial T}{\partial r} = h_i\,(T-T_f) \text{ in } r = r_i;\quad -K\frac{\partial T}{\partial r} = h_e\,(T-T_\infty) \text{ in } r = r_e;\quad \frac{\partial T}{\partial \phi} = 0 \text{ in } \phi=0 \text{ and } \phi=\pi \tag{2}$$

Making in (1) the change of variables:

$$r = r_i e^{\nu} = r_i R; \qquad \Theta = \frac{T-T_1}{T_2-T_1}, \tag{3}$$

equation (1) reduces to a simpler one in dimensionless form: $\frac{\partial^2 \Theta}{\partial \nu^2} + \frac{\partial^2 \Theta}{\partial \phi^2} = 0$ (4)

Assuming the classical separation of variables $\Theta(r,\phi) = N(\nu)\Phi(\phi)$ we obtain the following general solution for $\Theta(r,\phi)$ in a quite straightforward manner:

$$\Theta(R,\phi) = \sum_{n=0}^{\infty} N_n(\nu)\Phi_n(\phi) = A_o/2 + D_o \ln R + \sum_{n=1}^{\infty}(A_n R^n + B_n R^{-n})\cos n\phi \tag{5}$$

In order to obtain the coefficient A_n, B_n and D_o by using the boundary conditions (2-a,b), we assume that the dimensionless fluid temperature can be expanded as a cosine-Fourier series:

$$\Theta_f(\phi) = \frac{T_f(\phi) - T_1}{T_2 - T_1} = C_o/2 + \sum_{n=1}^{\infty} C_n \cos n\phi \tag{6}$$

For example, if Θ_f varies linearly with ϕ within the separating layer, the following expression applies for the coefficients C_n:

$$C_n = \int_0^{\pi} \Theta_f\,(\phi)\cos n\phi d\phi = -\frac{4}{\pi\varepsilon n^2}\sin n\phi_e \sin\frac{n\varepsilon}{2} \tag{7}$$

where ϕ_e and ε are defined in figure 1.

Defining now the internal and external Biot number respectively as follows:

$$B_i = \frac{h_i r_i}{K} \qquad B'_i = \frac{h_e r_i}{K} \tag{8}$$

and applying (2-a) and (2-b), after some algebraic work it results:

$$A_o = C_o + \frac{B'_i}{B_i}\cdot\frac{2\Theta_\infty - C_o}{(B'_i \ln R_e + 1/R_e + B'_i/B_i)};\quad D_o = \frac{B'_i(\Theta_\infty - C_o/2)}{(B'_i \ln R_e + 1/R_e + B'_i/B_i)} \tag{9}$$

$$A_n = \frac{B_i(B'_i R_e - n)C_n}{(B_i - n)(B'_i R_e^{-n}) - (B_i + n)(B'_i R_e^{2n+1} + n R_e^{2n})} \tag{10}$$

$$B_n = \frac{-B_i(B'_i R_e^{2n+1} + n R_e^{2n})C_n}{(B_i - n)(B'_i R_e - n) - (B_i + n)(B'_i R_e^{2n+1} + n R_e^{2n})} \tag{11}$$

In the assumption of adiabatic outer surface ($B'_i = 0$), the final expression for the dimensionless temperature simplifies significantly:

$$\Theta(R,\phi) = \frac{C_o}{2} + \sum_{n=1}^{\infty}\frac{C_n(R^n + R_e^{2n}.R^{-n})}{(1-\frac{n}{B_i}) + (1+\frac{n}{B_i})R_e^{2n}}\cos n\phi \tag{12}$$

As an illustrative example, the temperature distributions on the inside and outside bounding surfaces of a tube wall with $R_e = 1.1$ for a particular separating layer are shown

in figure 2, taken the internal Biot number as the parameter.

4. Calculation of the thermal stress distribution

According to hypotheses 6) and 7) of Section 2, the displacement axial component w of an arbitrary point (x, y, z_A) belonging to a given section $z = z_A$ of the tube, depends (linearly) only on the y - coordinate, whereas the vertical component v is constant (see figure 3):

$$w = w_o - \frac{dv}{dz}\, y \quad ; \quad v = v_o \tag{13}$$

w_o and v_o are the displacement components of the point at the neutral axis (0, y_o, z_A).

The longitudinal strain at this point will then be:

$$\varepsilon_z = \frac{dw}{dz} = \frac{dw_o}{dz} - \frac{d^2v}{dz^2}\, y = \varepsilon_{zo} - \frac{d^2v}{dz^2}\, y \tag{14}$$

being $\varepsilon_{zo} = dw_o/dz$ the longitudinal strain of the neutral axis. Knowing ε_z, the longitudinal stress (main unknown of our problem) is immediately obtained from Hooke's Law:

$$\sigma_z = E\,(\varepsilon_z - \alpha T) = E\,(\varepsilon_{zo} - \frac{d^2v}{dz^2}\, y - \alpha T) \tag{15}$$

The unknown coefficients ε_{zo} and d^2v/dz^2 may be obtained by applying hypotheses 8) of Section 2, which implies that the total force and moment at the given section $z = z_a$ are both null:

$$M_x = \int_\Omega \sigma_z y \, d\Omega = 0 \; ; \; N_z = \int_\Omega \sigma_z \, d\Omega = 0 \tag{16}$$

where Ω is the cross-section of the tube at $z = z_A$.

Introducing Eq. (15) into the first one of (16), and taken into account that

$$\int_\Omega y \, d\Omega = 0, \tag{17}$$

we immediately obtain:

$$\frac{d^2v}{dz^2} = -\frac{1}{I_x} \int_\Omega \alpha\, T\, y \, d\Omega \quad ; \quad I_x = \int_\Omega y^2 \, d\Omega \tag{18}$$

In a similar way, an expression for ε_{zo} results by introducing Eq. (15) into the second one (16), and using (17)

$$\varepsilon_{zo} = \frac{\int_\Omega \alpha\, T \, d\Omega}{\int_\Omega d\Omega} = \frac{1}{\Delta} \int_\Omega \alpha\, T \, d\Omega \tag{19}$$

From (15), (18) and (19) results a general expression for the longitudinal stress induced by thermal stratification:

$$\sigma_z(r,\phi) = E\left(\frac{1}{\Delta} \int_\Omega \alpha\, T \, d\Omega + \frac{y}{I_x} \int_\Omega \alpha\, T \, d\Omega - \alpha\, T\right) \tag{20}$$

Because analytical solution of the thermal field is known, solving the integrals in (20) we can obtain the corresponding analytical solution of the stress distribution. For the common case of adiabatic boundary condition at the outer surface ($B'_i = 0$) in which Eq. (12) applies, and assuming linear variation of θ with ϕ within the separating layer, we arrive to the following solution after some algebraic manipulations:

$$\frac{\sigma_z}{E\,\alpha(T_2 - T_1)} = \frac{C_1}{(1 - \frac{1}{B_i}) + (1 + \frac{1}{B_i}) R_e^2} \cdot R_e^2 \left[\frac{2R}{R_e^2 + 1} - \frac{1}{R}\right] - \sum_{n=2}^{\infty} \frac{C_n (R^n + R_e^{2n} R^{-n})}{(1 - \frac{n}{B_i}) + (1 + \frac{n}{B_i}) R_e^{2n}} \cos n\,\phi \tag{21}$$

The variation of the stress profile with the level of a zero-thickness separating layer, calculated by Eqs. (21) and (7) for a tube of $R_e = 1.1$ and $B_i = \infty$, is shown in figure 4.

Because this layer may change its position (given by ϕ_e) with time, the magnitude of interest for a fatigue analysis is the maximum stress intensity range for every point at the inside surface (defined by its ϕ-coordinate). It is equal to the difference between both envelope curves indicated in figure 4, determined by the maximum and minimum values of Eq. (21) varying ϕ_e in Eq. (7) from 0 to 180°. Taking ϕ as fixed in Eq. (21), this limit values can be obtained by calculating the zeros of the non-linear algebraic equation:

$$\frac{\partial}{\partial \phi_e} \frac{\sigma_z}{E\alpha(T_2-T_1)} = \sum_{n=1}^{\infty} \frac{\partial}{\partial C_n} \frac{\sigma_z}{E\alpha(T_2-T_1)} \cdot \frac{\partial C_n}{\partial \phi_e} = 0 \qquad (22)$$

It is clear from Eq. (22) that its left-hand-side results from substituting the coefficients C_n in Eq. (21) by its derivates respect to ϕ_e:

$$\frac{\partial C_n}{\partial \phi_e} = - \frac{4}{\pi \varepsilon n} \cos n\phi_e . \sin \frac{n\varepsilon}{2} \qquad (23)$$

The influence of the internal Biot number on both envelope curves, as calculated in the above manner, are shown in figure 5.

5. Estimation of the thermally induced stress intensity factor for circumferential flaws

Estimations of the stress intensity factor K_I induced by the above stress field, for flaws normal to the tube axis as indicated in figure 6, can be obtained by using the procedure proposed in the ASME Code, Section XI, Appendix A [16]. Neglecting the curvature of the tube wall, the following expression applies:

$$\frac{K_I}{E\alpha(T_2-T_1)\sqrt{\pi a}} = \frac{1}{\sqrt{Q_o}} \cdot \frac{M_m \sigma_m + M_b \sigma_b}{E\alpha(T_2-T_1)} \qquad (24)$$

where $Q_o(a/c)$ is the flaw shape parameter regardless plasticity effects, given by:

$$Q_o = 1 + 4.593\ (a/2c)^{1.65}\ ;$$

σ_m and σ_b are the membrane and bending components of σ_z; and $M_m(a/c,a/t)$, $M_b(a/c,a/t)$ are the membrane and bending stress correction factors respectively, given by figures A-3300-3 and A-3300-5 of ref. 16.

Relations between the flaw length and the flaw depth, shown in figure 7, have been chosen so that calculated stresses at points A and B of the flaw (see figure 6) would have the same stress in the absence of flaw. In the left hand side of figure 6, variations with ϕ_e and B_i of the calculated stress intensity factor are plotted. Finally, the maximum value of K_I in terms of a/t and B_i are indicated in figure 8.

References

1. S.H.Bush: "Pressurized water reactors". IAEA-SM-269/73, pp. 29-56.
2. D.Burkhart: "Swedes repair BWR thermal fatigue cracks". Nuclear Engineering International, June 1981, pp. 25-27.
3. J.Varley: "Feedwater pipework replaced at Ringhals 1". Nuclear Engineering International, Vol.27, N°324, March 1982, pp. 21-26.
4. K.Kussmaul, D.Blind and J.Jansky: "Safety analysis of circumferentially cracked feed water piping of light water reactors". SMIRT-7 Post-Conference Seminar "Assuring Structural Integrity of Steel Reactor Pressure Boundary Components", Chicago, Illinois, USA, Aug. 22-26, 1983.

5. A.F.Iorio and J.C.Crespi: "Analysis of the failure performance of internally pressurized piping with surface flaws". Int.Journal of Pressure Vessels and Piping, 9 (1981) pp.241-250.

6. J.Porto and G.Sánchez Sarmiento: "Analysis of the main causes of failures in the Atucha I PWR moderator circuit branch piping", International Meeting on Thermal Nuclear Reactor Safety, Chicago, Illinois, U.S.A., Aug.29-Sept.2, 1982.

7. M.Miksch, E.Lenz and R.Löhberg: "Loading conditions in horizontal feedwater pipes of LWRs influenced by thermal shock and thermal stratification effects". 9.MPA-Seminar, October 13 and 14, 1983. Staatliche Materialprüfungsanstalt Universitat Stuttgart, F.R.Germany.

8. R.Braschel, M.Miksch and G.Schücktanz: "Thermal stratification in steam generator feedwater lines". Pressure Vessel and Piping Conference, Orlando, Florida, U.S.A., June 27-July 2, 1982.

9. S.R.Idelsohn and L.E.Costa: "Thermal stratification as a cause of failures in the moderator circuit of a PHWR: Finite element analysis". Submitted for publication (1984).

10. M.Goldstein, H.Palamidessi and J.Porto: "Test models and solutions for moderator circuit failure in the PHWR Atucha I". IAEA Specialists' Meeting on Experimental and Modelling Aspects of Small-break LOCA, Budapest, Hungary, October 3-7, 1983.

11. Berkefeld and Gailer: "Analytische Berechnungsverfahren zur Ermittlung der Axialspannungen infolge Schichtung an einem Rohrquerschnitt unter Berücksichtigung von Mischzonen". KWU-Arbeits Bericht, R213/555/81. Erlangen, 11.12.81.

12. Dawel and Schiffer: "Parameter studie zur Ermittlung der Einflüsse von Steiggeschwindigkeit und Mischzone auf Schichtungsspannungen in Rohrquerschnitt". KWU-Arbeits Berich R213/567/81. Erlangen, 11.12.81.

13. Schön: "Analytische Berechnungsverfahren zur Ermittlung der Axialspannungen infolge Schichtung an einen Rohrquerschnitt". KWU-Arbeits Bericht R213/175/82. Erlangen, 27.04.82.

14. J.H.Cutrim and Kizivat: "A simplified method to calculate the stresses in straight pipes due to laminar flow of a stratified medium with two different temperatures". KWU-Work Report R622/83/16. Offenbach, 07.02.83.

15. J.L. de França Filho, H.Santos Souza and S.Guerreiro Ribeiro: "A practical case of piping deformation caused by transversal and longitudinal thermal gradient". (In portuguese). II Simposio Brasileiro sobre Tubulações e Vasos de Pressão. Salvador, BA, Brasil, Nov. 24-26, 1982.

16. Boiler and Pressure Vessel Code, Section XI, Rules for In-service Inspection of Nuclear Power Plant Components. Division 1, Appendix A (Analysis of Flaw Indications). American Society of Mechanical Engineering, 1980 Edition.

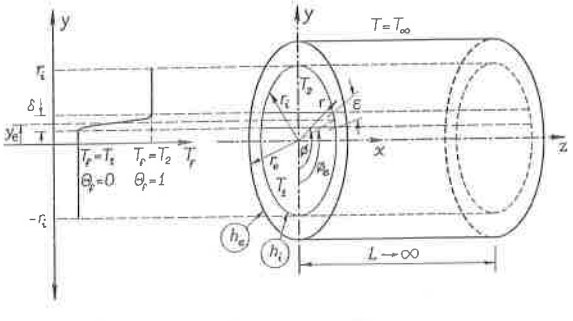

Figure 1 : Geometry of the problem under study and temperature distribution in the fluid.

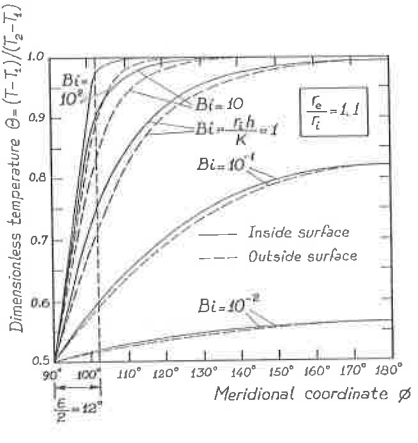

Figure 2 : Temperature of inside and outside bounding surfaces of the tube calculated according to Eqs. (12) and (7) for $y_e = 90°$, $\varepsilon = 24°$ and $r_e/r_i = 1.10$, and varying the internal Biot number.

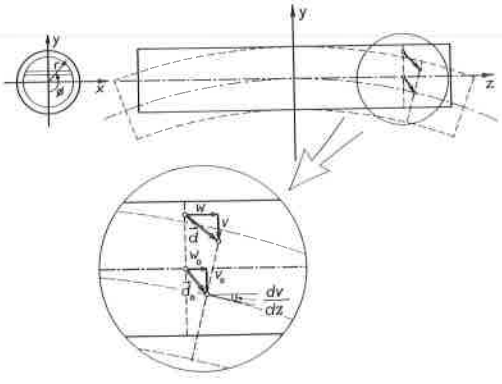

Figure 3 : Scheme of the tube deformation induced by thermal stratification.

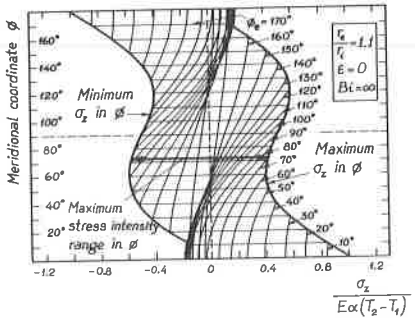

Figure 4 : Dimensionless axial stress induced by the thermal stratification, as calculated by Eqs. (21) and (7) in terms of the position ϕ_e of the separating layer.

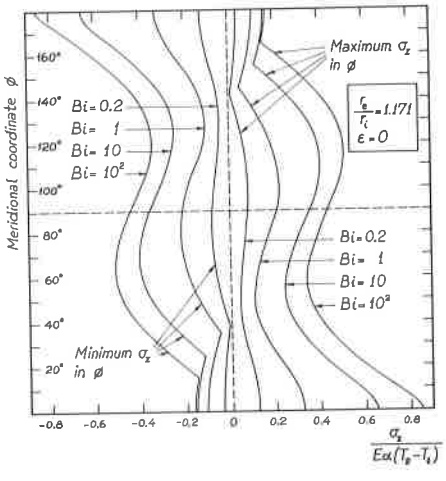

Figure 5 : Influence of the internal Biot number on the dimensionless thermal axial stress calculated according to Eqs. (21) and (7).

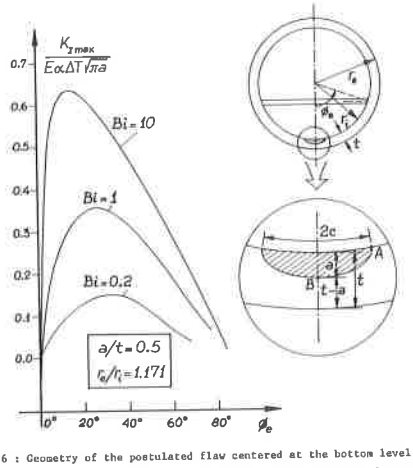

Figure 6 : Geometry of the postulated flaw centered at the bottom level, and variations with ϕ_e and B_1 of the stress intensity factor calculated according to Eqs. (24), (7) and (21).

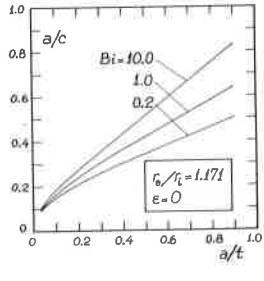

Figure 7 : Calculated relations between the flaw length and the flaw depth.

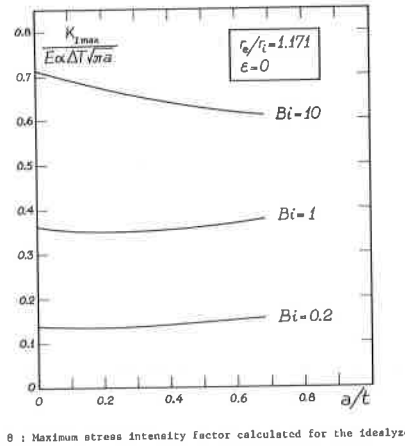

Figure 8 : Maximum stress intensity factor calculated for the idealyzed flaws of figure 6, in terms of the flaw depth and the internal Biot number.